

**Conference on**  
**Machine Processing of**  
**Remotely Sensed Data**

**October 16 - 18, 1973**

The Laboratory for Applications of  
Remote Sensing

Purdue University  
West Lafayette  
Indiana

Copyright © 1973  
Purdue Research Foundation

This paper is provided for personal educational use only,  
under permission from Purdue Research Foundation.

## MULTITEMPORAL GEOMETRIC DISTORTION CORRECTION

### UTILIZING THE AFFINE TRANSFORMATION

R. A. Emmert and C. D. McGillen

Lawrence Livermore Laboratory, Livermore, California;  
Laboratory for Applications of Remote Sensing, Purdue  
University, West Lafayette, Indiana

#### I. ABSTRACT

In the analysis of multitemporal remotely sensed imagery, it is necessary to place these data into registration. To implement this operation the data are divided into subimages, and the misregistration between the data subsets is modeled by an affine transformation. The properties of the Fourier transform of a two-dimensional function under the affine transformation are given, and examples of these relations between the spatial and spatial frequency domains are shown. Techniques for the estimation of the coefficients of the distortion model using the spatial frequency information are developed, and an example of the use of this method for the correction of line scanner imagery is given.

#### II. INTRODUCTION

In analyzing imagery obtained by remote sensing devices, it is frequently necessary to compare data taken at different times on a point by point basis. In order to carry out such a comparison, it is necessary to register, or overlay, one set of data on the other. Thus, it is required to process one set of data such that its image under an appropriate transformation is in proper geometrical registration with the other data.

Before implementing a registration operation, a model characterizing the misregistration must first be introduced, and the choice of the size of the data set for which the model is to be valid determines its complexity. If a large data set is chosen, the resulting model is most often complex. However, if the data are divided into smaller subimages, or regions, the resultant model for each of these regions is simple.

In this study the misregistration between data regions is modeled by an affine transformation, and the properties of the Fourier transform of a two-dimensional function under this transformation are given. The coefficients of the geometrical distortion component of this model are readily estimated in the spatial frequency domain, and an example of the use of spatial frequency information for the correction of distortion in line scanner imagery is given.

#### III. A REGIONAL MISREGISTRATION MODEL

A general model for characterizing misregistration between two sets of remotely sensed data is the two-dimensional polynomial

$$y_i = \sum_{j=0}^{N-1} \sum_{k=0}^{N-1} a_{jk} x_1^j x_2^k, \quad i = 1, 2 \quad (1)$$

where  $x$  and  $y$  are respectively the coordinate systems of the arbitrarily chosen reference and background data sets. This model is useful because the linearity of the equations as a function of the coefficients permits least-squares procedures to be used for determining these coefficients. Table

1 lists several polynomials obtained from this model and includes the number of coefficients that would be required to utilize the corresponding model.

For many data sets regional misregistration can be represented as having the following four components: (1) scale, (2) rotation, (3) skew, and (4) displacement. Such misregistration can be completely characterized by means of the affine transformation given by

$$\underline{y} = \underline{H} \underline{x} = \underline{A} \underline{x} + \underline{t}$$

where

$$\underline{y} = \begin{bmatrix} y_1 \\ y_2 \end{bmatrix}, \quad \underline{x} = \begin{bmatrix} x_1 \\ x_2 \end{bmatrix}, \quad \underline{t} = \begin{bmatrix} t_1 \\ t_2 \end{bmatrix} \quad (2)$$

and

$$\underline{A} = \begin{bmatrix} a_{11} & a_{12} \\ a_{21} & a_{22} \end{bmatrix} .$$

The non-singular matrix A characterizes the geometrical components of the misregistration. The quantities are illustrated in Fig. 1.

The usefulness of the affine model results from the fact that the misregistration can be interpreted as consisting of two components: the first is the characterization of the geometrical distortion by a linear model, and the second is the displacement of the coordinate systems. Straightforward search techniques are available for estimating the distortion matrix coefficients by determining the differences between the moduli of the Fourier transforms of these data.

#### IV. TWO-DIMENSIONAL FOURIER TRANSFORM UNDER AN AFFINE TRANSFORMATION

The two-dimensional Fourier Transform of the function  $f(\underline{x})$  is defined as

$$F(\underline{u}) = \int_{-\infty}^{\infty} \int_{-\infty}^{\infty} f(\underline{x}) \exp\{-j2\pi(\underline{u}, \underline{x})\} d\underline{x} \quad (3)$$

and the inverse is

$$f(\underline{x}) = \int_{-\infty}^{\infty} \int_{-\infty}^{\infty} F(\underline{u}) \exp\{j2\pi(\underline{u}, \underline{x})\} d\underline{u} \quad (4)$$

where

$$\underline{u} = \begin{bmatrix} u_1 \\ u_2 \end{bmatrix}$$

and the notations  $(\underline{u}, \underline{x})$  denotes the inner product of the vectors  $\underline{u}$  and  $\underline{x}$ . The following properties of the transform of the function  $f(\underline{x})$  under an affine transformation  $\underline{H}$  are readily established.

(1) Similarity

If

$$f(\underline{x}) \xrightarrow{\underline{H}} f(\underline{H} \underline{x}) = g(\underline{y}), \quad (5)$$

then

$$G(\underline{y}) = \mathfrak{F}\{f(\underline{H} \underline{x})\} = \frac{1}{|J|} \exp\{j2\pi(\underline{u}, \underline{A}^{-1} \underline{t})\} F\{(\underline{A}^{-1})^T \underline{u}\} \quad (6)$$

where

$$J = \frac{\partial(y_1, y_2)}{\partial(x_1, x_2)}$$

is the Jacobian of the transformation.

(2) Energy Spectrum and Modulus Independent of  $\underline{t}$

The energy density spectrum of  $f(\underline{x})$  is

$$S(\underline{u}) = |F(\underline{u})|^2, \quad (7)$$

and the linear phase term cancels. The modulus is

$$M(\underline{u}) = \{ |F(\underline{u})|^2 \}^{1/2} \quad (8)$$

and the result is immediate.

(3) Symmetry of the Modulus

For real signals it readily follows from (3) that

$$F(-\underline{u}) = F^*(\underline{u}) \quad (9)$$

where the asterisk denotes the complex conjugate.

(4) Relation of Coordinate Systems

From (6) it follows that the relation between coordinate systems  $\underline{u}$  and  $\underline{v}$  of the transform moduli is

$$\underline{v} = (\underline{A}^{-1})^T \underline{u} \quad (10)$$

#### V. ESTIMATION OF DISTORTION MATRIX COEFFICIENTS

In a number of special cases the distortion matrix  $\underline{A}$  reduces to a simpler form, and it is illustrative to examine the effects of various geometrical distortions in these domains. For scaling changes the distortion matrix is

$$\underline{A} = \begin{bmatrix} a_{11} & 0 \\ 0 & a_{22} \end{bmatrix} \quad (11)$$

where the scaling is assumed to be along the coordinate axes. The relationship between the spatial frequency domain coordinates is then

$$\underline{v} = (\underline{A}^{-1})^T \underline{u} = \begin{bmatrix} \frac{1}{a_{11}} & 0 \\ 0 & \frac{1}{a_{22}} \end{bmatrix} \underline{u} \quad (12)$$

This relation is illustrated in Fig. 2 where the dimensions of the rectangular blocks in the spatial domain have a width which is two times the height.

For rotation the distortion matrix is

$$\underline{A} = \begin{bmatrix} \cos \theta & \sin \theta \\ -\sin \theta & \cos \theta \end{bmatrix} \quad (13)$$

which is an orthogonal matrix. Thus

$$\underline{v} = (\underline{A}^{-1})^T \underline{u} = \underline{A} \underline{u} \quad (14)$$

and the transform of the distorted data is also rotated by the angle  $\theta$ ; this distortion is illustrated by the modulus of the transform of the ideal data shown in Fig. 3.

For skew distortion the geometric distortion matrix becomes

$$\underline{A} = \begin{bmatrix} 1 & 0 \\ a_{21} & 1 \end{bmatrix} \quad (15)$$

and in the spatial frequency domain the coordinates are related by

$$\underline{v} = \begin{bmatrix} 1 & -a_{21} \\ 0 & 1 \end{bmatrix} \underline{u} \quad (16)$$

This distortion and its associated modulus of the Fourier transform are shown in Fig. 4.

The overall distortion matrix  $\underline{A}$  is some combination of these component distortions.

The differences between the moduli of the transforms of two corresponding regions of data provide all the information required for determining values for the coefficients of the linear distortion matrix. The zero spatial frequency component is mapped into the origin of the transform domain and higher frequency components are mapped into locations proportional to both the value of their spatial frequency and in a direction from the origin characteristic of the orientation of the component in the spatial domain. The moduli of the two-dimensional Fourier transforms of corresponding regions of data are invariant under the coordinate shift  $\underline{t}$ ; thus the coordinate systems can be chosen arbitrarily. It is further assumed that for data of a reasonably homogenous composition, small shifts  $\Delta d$  of the data aperture will yield moduli which can be assumed to be unchanged for purposes of this study.

The class of agricultural imagery, which is of principal interest in this study, typically consists of a collection of rectangular fields with each of the fields having essentially a homogeneous ground cover. It has been observed that the modulus of the two-dimensional Fourier transform of a data set from this class of imagery typically exhibits a simple structure with the property that a majority of the energy in the spatial frequency domain is concentrated along linear loci or rays perpendicular to the field boundaries.

The rotative and skew components of the misregistration are obtained by determining the directions of the loci of energy maxima in each of the two transform moduli. From these angles it is then possible to compute the parameters of the transformation corresponding to the geometrical distortion in the images.

Referring to Fig. 5 the geometrical distortion matrix for skew and rotation only is given by

$$\underline{A} = \begin{bmatrix} \cos \phi_1 & \dagger \sin \phi_1 \\ a_{21} \cos \phi_1 \dagger \sin \phi_1, & \dagger a_{21} \sin \phi_1 \dagger \cos \phi_1 \end{bmatrix} \quad (17)$$

where

$$a_{21} = \cot(\theta_2 - \phi_1).$$

## VI. APPLICATION TO MEASURED DATA

As an example of the application of this technique, images obtained from an airborne multi-spectral scanner system on two different days have been analyzed and the geometrical distortion components determined. The area for which the correction was computed and the corresponding Fourier transform moduli are shown by Fig. 6. The fast Fourier transform algorithm was used for

computing the transform of these data. In each of these pictures the transformed data have a logarithmic amplitude scale, and the gray scale employed in the display system is linear. The size of the data set being transformed is 128 x 128 picture elements.

A regression line representing the best least-squares fit of the maxima of the modulus along a radial line was used to obtain the angle between each loci and its coordinate axis. The angular quantities given by this algorithm, measured with respect to the  $u_1$  axis, are as follows

data set A	$-7.18 \times 10^{-2}$ radian	
	1.57	"
data set B	$-3.30 \times 10^{-2}$	"
	1.52	"

With a hypothetical transform coincident with the coordinate axes used as a reference data transform, the resultant angular quantities defined in Fig. 5 are

data set A	$\phi_1 = -4.1^\circ$
	$\phi_2 = 0^\circ$
data set B	$\phi_1 = -1.9^\circ$
	$\phi_2 = -3.3^\circ$

The two-dimensional polynomial was used to implement the correction. Rather than mapping one data set into the other, it was chosen to rectify each data set. Examining the data sets in both the spatial and spatial frequency domain, the angular quantities chosen for the rectification differed slightly from those above. The numerical values used for the rectification are

data set A	$\phi_1 = -3.7^\circ$
	$\phi_2 = 0^\circ$
data set B	$\phi_1 = -1.7^\circ$
	$\phi_2 = -3.3^\circ$

with the reference transform angular quantities having the values

$$\theta_1 = 0^\circ$$

$$\theta_2 = 90^\circ$$

for each of the data sets.

The distortion matrices are then

$$\underline{A}_1 = \begin{bmatrix} 0.9979 & -0.0645 \\ 0.0 & 1.002 \end{bmatrix} \quad (18)$$

$$\underline{A}_2 = \begin{bmatrix} 0.9999 & -0.0297 \\ 0.0576 & 0.9987 \end{bmatrix} \quad (19)$$

The results of this geometrical correction on the spatial data are shown in Fig. 7. It is emphasized that the correction is applicable only in the center of each of these pictures as the distortion introduced by the aircraft motion is a dynamic quantity.

## VII. REFERENCES

Goodman, J. W., "Introduction to Fourier Optics," McGraw-Hill, New York, 1968.

Hadley, G., "Linear Algebra," Addison Wesley, Reading, 1961.

Lendaris, G. and G. Stanley, "Diffraction-Pattern Sampling for Automatic Pattern Recognition," Proc. IEEE, vol. 58, no. 1, pp. 198-216, February, 1970.

## VIII. TABLES AND ILLUSTRATIONS

Table 1. Two-Dimensional Polynomial Misregistration Models

Common Name	Degree N-1	No. Parameters To Be Determined
DISPLACEMENT	0	2
LINEAR	1	4
AFFINE	1	6
PROJECTION	2	8
QUADRATIC	2	12
CUBIC	3	20

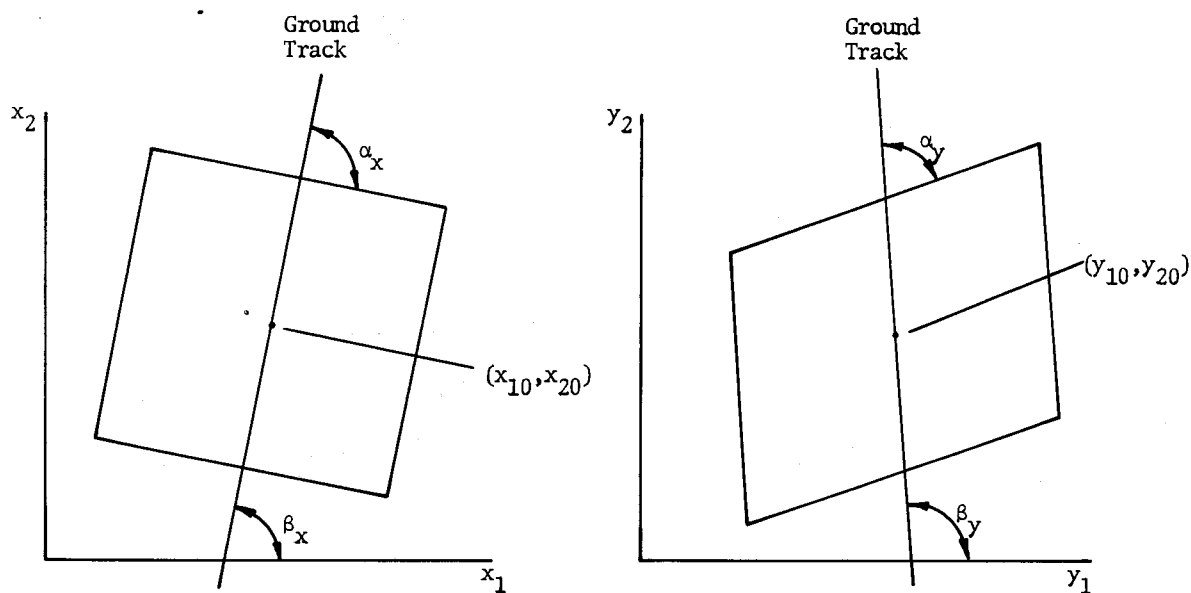
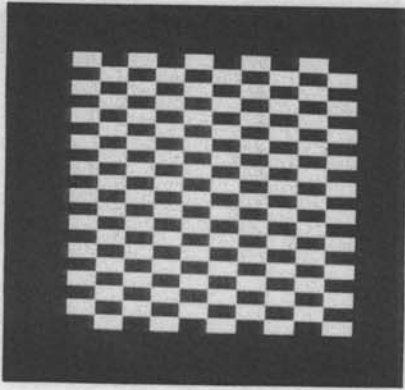
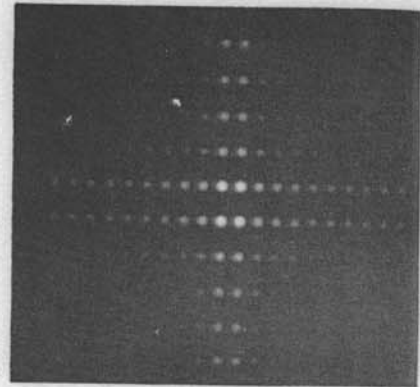


Figure 1. Misregistration Between Data Regions

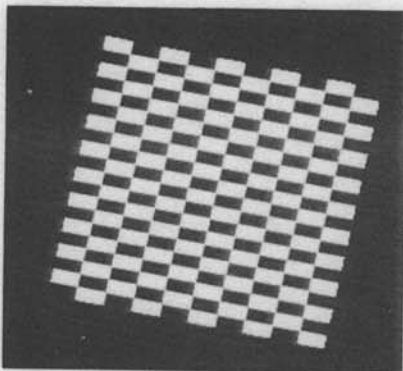


Block Pattern

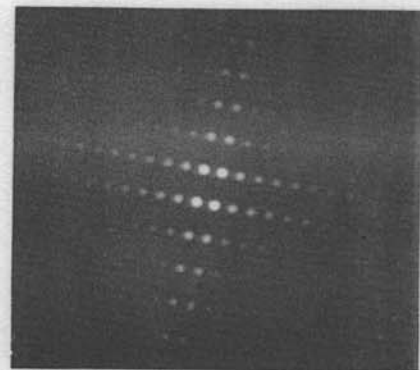


Modulus of Fourier Transform

Figure 2. Modulus of Fourier Transform of Block Pattern

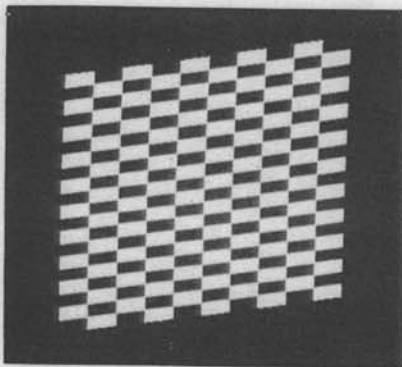


Rotated Block Pattern

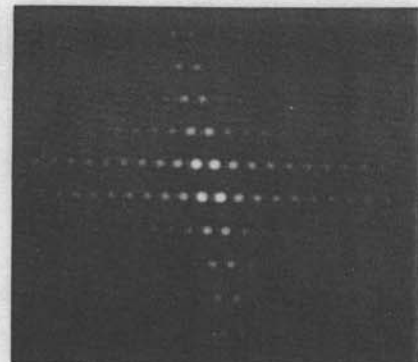


Modulus of Fourier Transform

Figure 3. Modulus of Fourier Transform of Rotated Block Pattern



Block Pattern with Skew



Modulus of Fourier Transform

Figure 4. Modulus of Fourier Transform of Skewed Block Pattern



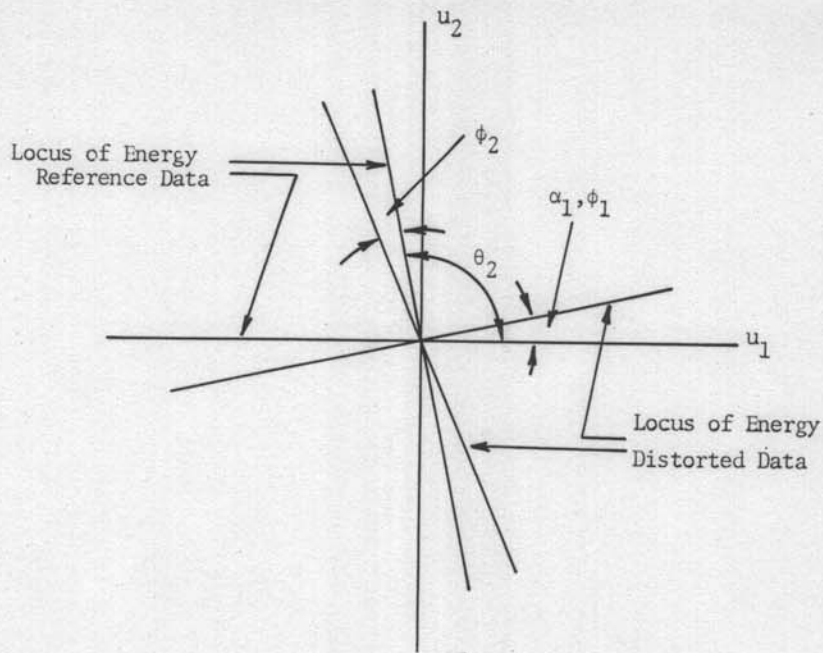


Figure 5. Location of Loci of Energy in the Modulus of the Two-Dimensional Fourier Transform, Rotational and Skew Distortion

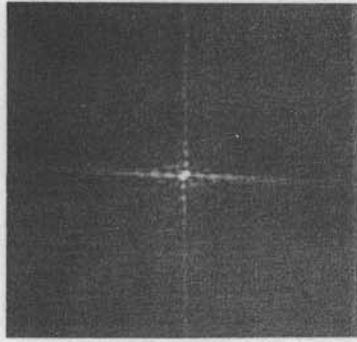


Data Set A

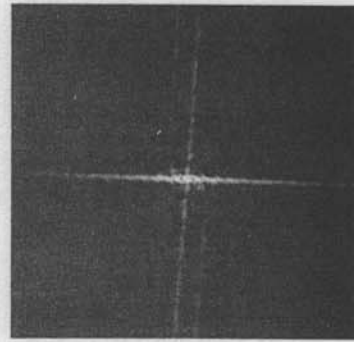


Data Set B

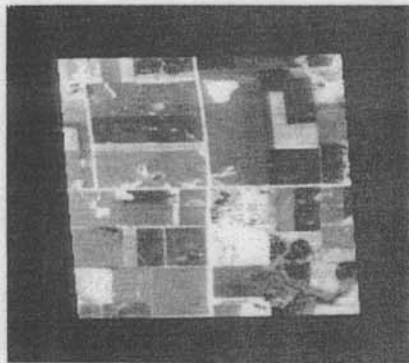
Figure 6. Multitemporal Imagery



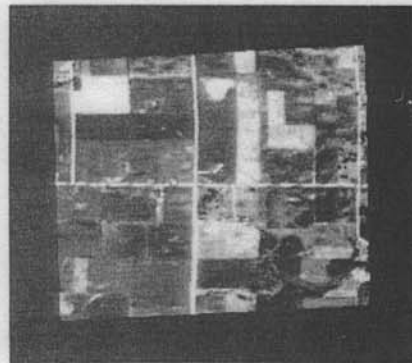
Data Set A



Data Set B



Data Set A



Data Set B

Figure 7. Modulus of Fourier Transform of Distorted Data and Geometrically Corrected Imagery